Persistent dynamic attractors in activity patterns of cultured neuronal networks

Daniel A. Wagenaar[*]

Department of Physics, California Institute of Technology, Pasadena, CA

Zoltan Nadasdy

Division of Biology, California Institute of Technology, Pasadena, CA

Steve M. Potter[†]

Laboratory for Neuroengineering, Coulter Department of Biomedical Engineering,

Georgia Institute of Technology and Emory University, Atlanta, GA

Abstract

Three remarkable features of the nervous system—complex spatiotemporal patterns, oscillations and persistent activity—are fundamental to such diverse functions as stereotypical motor behavior, working memory, and awareness. Here we report that cultured cortical networks spontaneously generate a hierarchical structure of periodic activity with a strongly stereotyped population-wide spatiotemporal structure demonstrating all three fundamental properties in a recurring pattern. During these 'superbursts', the firing sequence of the culture periodically converges to a dynamic attractor orbit. Precursors of oscillations and persistent activity have previously been reported as intrinsic properties of the neurons. However, complex spatiotemporal patterns that are coordinated in a large population of neurons and persist over several hours—and thus are capable of representing and preserving information—cannot be explained by known oscillatory properties of isolated neurons. Instead, the complexity of the observed spatiotemporal patterns implies large-scale self-organization of neurons interacting in a precise temporal order even *in vitro*, in cultures usually considered to have random connectivity.

---

[*]Present address: Division of Biological Sciences, University of California at San Diego, La Jolla, CA.

[†]Corresponding author. Email: steve.potter@ece.gatech.edu.

I. INTRODUCTION

In models of neural networks, attractor dynamics displaying complex reverberations emerge naturally if there are sufficient feedback connections [1–3]. Donald Hebb proposed that such reverberations may be used to encode and maintain information in the nervous system [4]. Recurring short spatiotemporal patterns of action potentials recovered from simultaneous recordings of multiple neurons *in vivo*, variously called 'sequences' [5, 6], or 'synfire chains' [7], may be subsamples of such dynamics. Recurring spatiotemporally complex activity patterns has been observed in sensory systems [8], where they have been described in terms of attractor dynamics [9], as well as in motor systems [10]. There is increasing evidence that even *in vitro*, excised brain slices can repeatedly express patterns of activity that are conserved for minutes or hours [11–14].

To test whether specific cortical microstructure is required for the emergence of precise spatiotemporal activity, we studied the activity of cortical neurons in dissociated culture. Neurons in dissociated culture retain many basic physiological properties, but do not develop the typical layered columnar organization of cortical tissue *in vivo*. The electric activity of such cultures is dominated by culture-wide bursts of high-frequency action potential firing, separated by periods of low firing rates [15–19]. Bursting in culture is reminiscent of bursting observed *in vivo* in the developing cortex [20] and elsewhere in the developing nervous system [21], as well as of sleep spindles in the thalamic reticular nuclei [22] and subthalamic nucleus during slow wave activity [23]. Here we report how at certain stages of development burst patterns have a precisely defined spatiotemporal structure that recurs with great fidelity over an interval of many hours. This shows that dissociated cortical networks in culture are capable of generating complex stereotypical behaviors that were previously believed to require specific network architecture.

II. METHODS

A. Cell culture

Dense cultures of rat cortex were prepared on multi-electrode arrays (MEAs; a list of abbreviations appears at the end of this paper) as described before [19, 24]. Briefly, cortices from E18 rat embryos were dissected and dissociated using papain and trituration.

Cells—neurons and glia—were plated at a density of $2500/mm^2$, on MEAs coated with poly-ethylene-imine (PEI) and laminin. Cultures were maintained in a serum-containing DMEM-based medium. We recorded daily from 30 cultures from day 3 to day 35 *in vitro*. Five cultures were followed for 2–3 days continuously.

B. Data analysis

1. Spike detection and sorting

Electrical signals from 59 electrodes were sampled at 25 kHz. Putative spikes were detected by thresholding the electrode traces at 4.5× estimated RMS noise. Double detection of multiphasic spikes was prevented by discarding candidate spikes in a ± 0.5 ms window around spikes of larger amplitude.

Most subsequent analysis was performed using multi-unit activity, obtained from 59 electrodes in a square grid with 200 μm spacing. In two cultures, we analyzed single-unit activity, obtained by using an unsupervised spike sorting method [25] with cross- and autocorrelation verification. Only the largest four spike clusters per electrode (i.e., four neurons with highest firing rates) were included in the data analysis. To ensure stability of clusters over time, the sorting was done in data segments of 400 s with 40 s overlaps. The redundant clustering on the overlaps allowed us to match spike clusters consistently across segments. Spike clusters were tested for refractoriness. In both cultures the sorting resulted in 236 putative neurons (59 electrodes × 4 clusters).

Cross-correlation analysis revealed that inter-electrode spacing was such that cells did not evoke potentials on more than one electrode. This also implied that using multi-unit data does not compromise the spatial resolution of the analysis.

2. Burst identification

Bursts were detected by means of the SIMMUX algorithm [26]. Briefly, each electrode trace was searched for *burstlets*: sequences of at least four spikes with all inter-spike intervals less than a threshold (set to 1/4 of that electrode's inverse average spike detection rate, or to 100 ms, whichever was less). Any group of burstlets across several electrodes that overlapped in time was considered a *burst*.

3. Similarity Indices

A superburst similarity index (S_{super}) was computed based on the (multi-unit) firing rate summed over all electrodes. For each superburst n, we computed this firing rate, $f_n(t)$, in 50 ms (Gaussian) sliding windows (sampled at 500 Hz). $f_n(t)$ was set to zero for $t < 0$ or $t >$ (the duration of superburst n). The similarity index $S_{\text{super}}(n, m)$ between two superbursts n and m was then defined as the correlation coefficient between the functions f_n and f_m, optimally time-shifted:

$$
S_{\text{super}}(n, m) = \max_{\tau} \left(\frac{\int \left(f_n(t) - \overline{f_n} \right) \left(f_m(t + \tau) - \overline{f_m} \right) dt}{\sqrt{\int \left(f_n(t) - \overline{f_n} \right)^2 dt} \sqrt{\int \left(f_m(t) - \overline{f_m} \right)^2 dt}} \right),
$$

where $\overline{f_n}$ is the average of $f_n(t)$ over the duration of the superburst.

A subburst similarity index (S_{sub}) was based on the times at which individual electrodes started to record bursts. The onset time $t_{\text{on}}^c(n, k)$ of electrode c in the kth subburst of the nth superburst was defined as the moment when the baseline-substracted firing rate first increased to 25% of its peak during that subburst. (This use of relative thresholds ensured that differences in firing rates between electrodes did not cause a systematic bias in onset time estimation. We tested the independence of onset time estimates and firing rates by calculating the Pearson correlation coefficient, and found it was negligible ($r = -0.05$, $p = 0.13$; $N = 845$).) The similarity index $S_{\text{sub}}(n_1, k_1; n_2, k_2)$ between two subbursts (n_1, k_1) and (n_2, k_2) was then defined as the correlation coefficient between onset times across electrodes:

$$
S_{\text{sub}}(n_1, k_1; n_2, k_2) = \frac{\sum_c \left(t_{\text{on}}^c(n_1, k_1) - \overline{t_{\text{on}}}(n_1, k_1) \right) \left(t_{\text{on}}^c(n_2, k_2) - \overline{t_{\text{on}}}(n_2, k_2) \right)}{\sqrt{\sum_c \left(t_{\text{on}}^c(n_1, k_1) - \overline{t_{\text{on}}}(n_1, k_1) \right)^2} \sqrt{\sum_c \left(t_{\text{on}}^c(n_2, k_2) - \overline{t_{\text{on}}}(n_2, k_2) \right)^2}},
$$

where $\overline{t_{\text{on}}}(n_i, k_i)$ is the mean onset time of the k_i^{th} subburst of the n_i^{th} superburst across electrodes. Only electrodes with peak firing rates of at least 75 spikes per second were used in this calculation (typically: 40 electrodes).

4. Return plots

We performed return plot analysis on the onset latencies of individual electrodes in successive bursts, defined as $\lambda_{n,k}^c \equiv t_{\text{on}}^c(n, k) - \overline{t_{\text{on}}}(n, k)$. After spike sorting, we repeated this

4

analysis at the level of single neurons. Return plots elucidate higher order temporal relationship between successive events, by recursively plotting the latency of the nth event against the latency of the $n+1^{\text{st}}$. The appearance of clusters in return plots indicates a conserved temporal pattern in successive events, and the spread of clusters reflects the precision of conservation. When comparing return plot correlation coefficients at electrode level with those at single cell level, we balanced the sample size by random sub-sampling the population spikes. Thus we obtained an unbiased estimate of reproduction fidelity.

III.   RESULTS

Bursting in dissociated cultures commenced after 5–8 days *in vitro* (Figure 1), and persisted throughout a culture's lifetime (over one year [24]). During most of a culture's life, burst patterns were relatively unstructured. Burst frequencies ranged from 1 to 30 per minute, and appeared to be generated by a Poisson-like process modulated by a refractory period of 1 to 5 seconds. However, a majority of cultures (18 out of 30 cultures followed) passed through a developmental period lasting 3–5 days during the 2nd week *in vitro*, during which burst patterns acquired a large degree of structure. During such epochs, bursts occurred in sequences of 5 to 12, with inter-burst intervals of 2 to 4 seconds (Figure 2(a) and Movie 1 [45]). These sequences, which we call 'superbursts,' were separated by 1 to 10 minutes with a steady low firing rate (< 0.2 spikes/electrode/second). In contrast, the firing rate of the cells increased almost 100-fold when transitioning from non-bursting to bursting mode, implying that population-wide interactions of neurons were only enabled during the bursting phases. The intervals between superbursts were consistent with a Poisson process modulated by refractoriness (Figure 2(b)). In contrast, the intervals between the constituent bursts ('subbursts') within superbursts were highly stereotyped (Figure 2(c)). The number of bursts per superburst was likewise strongly conserved over long periods of time, though it varied considerably from culture to culture. As for the constituent bursts themselves, the first burst in a superburst typically contained the largest number of spikes, followed by a gradual decline, due to a reduction in the number of participating neurons. Remarkably, single-neuron firing rates remained nearly constant during most of the superburst (Figure 2(d)). In Figure 2 as well as in the following, we concentrate on results obtained from the longest recorded superburst epoch (63 hours). Results from all extended recordings are
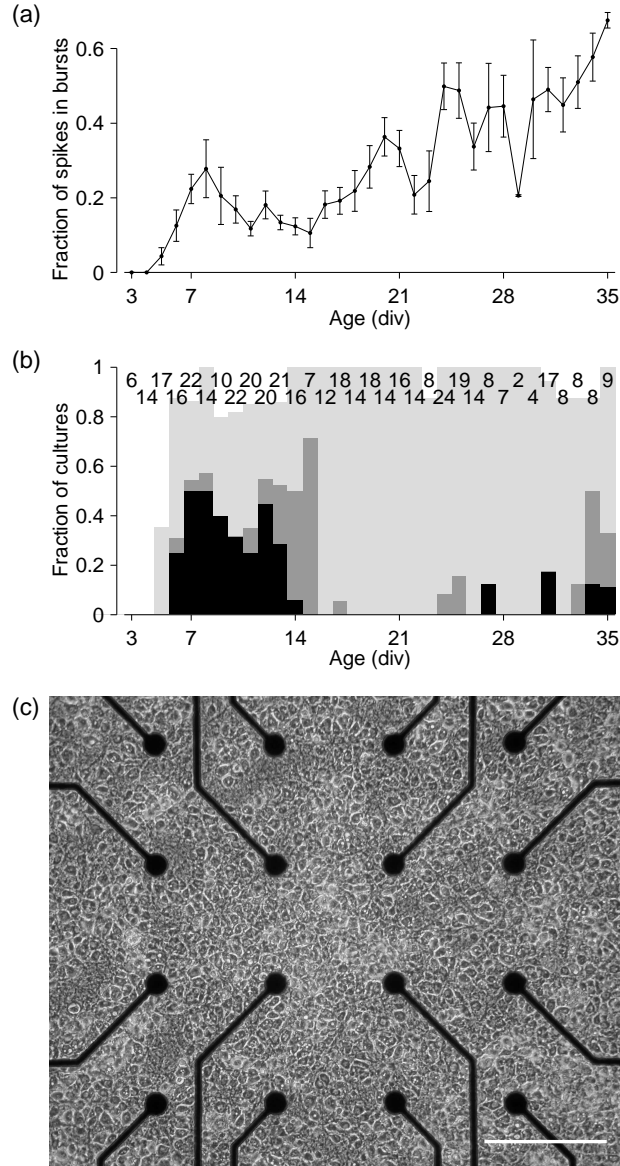
Figure 1: Development of bursting. (a) The fraction of spikes that occur in large bursts (rather than during tonic dispersed firing) grows with culture age (measured in days *in vitro* (div)). Here, 'large' means at least 5 participating sites with a total of at least 50 spikes. (b) Fraction of cultures that fire superbursts exclusively (black) or superbursts mixed with other bursts (dark gray). Light gray indicates fraction of cultures that exhibits any kind of bursts. Numbers on top indicate number of cultures studied at each age. (c) Phase contrast micrograph of a superbursting culture at 9 div. Scale bar: 200 μm.

Table I: Compendium of parameters for all five extended recordings.

	Culture No. 1	No. 2	No. 3	No. 4	No. 5
Age (div)	10	19	9	8	12
Duration of superbursting (hr)	63	11[a]	41	49	3[a]
Number of superbursts	292	49	94	154	24
Average number of subbursts	7	12	3	7	5
Superburst similarity index S_{super} (see text)	0.89	0.81	0.73	0.76	0.81

[a] These cultures were still superbursting when the recording was terminated.

summarized in Table I.

The overall structure of superbursts in any given culture persisted for hours, and any changes were usually discontinuous. To quantify this observation, we measured the array-wide aggregate of the firing rate in 50-ms sliding windows. This yielded a firing rate profile for each superburst (Figure 3(a)). We defined a 'superburst similarity index', S_{super}, between a pair of superbursts as the correlation coefficient between their firing rate profiles (aligned to maximize S_{super}, but not time-warped; see *Methods*). The similarity index between consecutive superbursts was very high (>90% on average), and remained high (>80%) between pairs of superbursts separated by dozens of other superbursts (Figure 3(c)). The matrix form of S_{super} of our longest recording is characterized by a block-diagonal structure, indicating that changes in the temporal structure of population firing during superbursts occurred in discrete steps of varying size (Figure 3(b)).

Like the global activity profile, the spatiotemporal dynamics of the activity spreading across the culture were also preserved within and across superbursts. We quantified this by the relative times at which individual electrodes started to record each subburst, and combining those into a (59-dimensional) vector, which constitutes an 'onset-time profile' for the subburst. We defined a 'subburst similarity index', S_{sub}, as the correlation coefficient between pairs of such vectors (see *Methods*). This revealed considerable similarity between subbursts within a superburst, particularly between the 2nd to 5th subbursts (Figure 3(d)). Moreover, homologous (like-numbered) subbursts had very similar onset profiles between consecutive superbursts (Figure 3(e)). Between the 2nd to 5th subbursts, this 'inter-superburst' S_{sub} exceeded the 'intra-superburst' S_{sub}. Comparing pairs of superbursts with
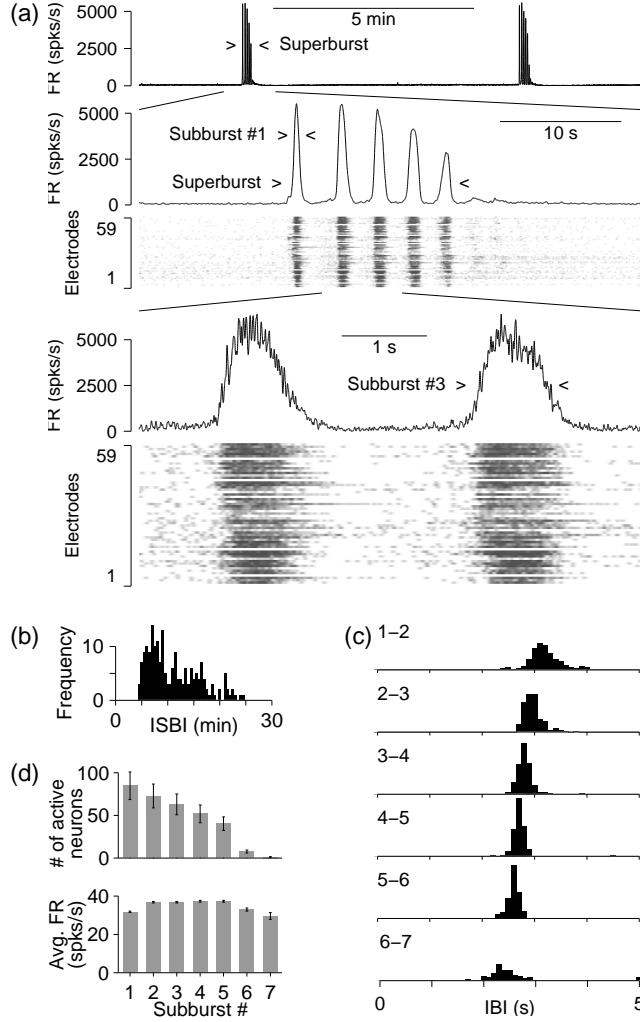
Figure 2: (a) An example of a 10 minute data segment illustrates the typical two-level temporal organization of population activity in superbursts. Firing rates (FR) are culture-wide aggregates. Simultaneous raster plots from 59 electrodes reveal that nearly all electrodes record from neurons participating in this structure. Note that the beginning of each burst occurs at slightly different times at different electrodes, defining a characteristic onset-time profile. This is further explored in Figure 3(d–e). (b) The distribution of intervals between 195 superbursts recorded over a 35 hour period (inter-superburst intervals; ISBI). (c) The distributions of the intervals between subbursts within superbursts (inter-burst intervals; IBI). Histograms show all subburst intervals at a fixed ordinal position (indicated on top-left) in their superbursts. (d) Number of active neurons (top) and average firing rate per active neuron (bottom), per subburst. Spike sorting was performed using super-paramagnetic clustering [25].

more time between them, the S_{sub} index between the 1st subbursts was much reduced, indicating a gradual change of the state of the network. In striking contrast, the S_{sub} index between the 2nd to 5th subbursts remained high, indicating that, despite this gradual change, the superburst attractor is conserved, and that the attractor trajectory can be reached from many different initial conditions.

For another view of the dynamics of burst onset, we constructed return plots of the onset latencies of individual electrodes both between consecutive subbursts within a superburst, and between homologous subbursts of successive superbursts. After spike sorting, analogous plots were constructed at the single-cell level, to help determine whether the activity of specific neurons was crucial to the structure of superbursts. If individual neurons play conserved roles in different bursts, their relative burst onset latencies should be conserved from burst to burst, causing the latencies to line up along the diagonal of the return plot. Moreover, the latencies of an individual cell should cluster in a confined region along the diagonal. Both effects are indeed evident in Figure 4. The relative latencies of different electrodes were consistent across successive component bursts ($r = 0.55$; $p < 0.01$; Figure 4(a)). Individual neurons engage in the successive bursts with similarly precise latency relative to other neurons ($r = 0.58$; $p < 0.01$; Figure 4(b)). A neuron that started bursting earlier than the population would always be earlier than a neuron that started bursting later (Figure 4(c)). The gross conservation of latencies was complemented by a systematic drift in the onset latencies for a given neuron across successive component bursts (Figure 4(d)). Relative onset latencies of different neurons were also strongly preserved between homologous components of consecutive superbursts ($r = 0.57$; $p < 0.01$; Figure 4(e)). The observation that the latency profile is consistent across subbursts and superbursts implies that the transition from tonic to burst-firing propagates across the culture following a similar path each time. Since the burst onset order at cellular level was slightly more consistent than at electrode level ($r = 0.58$ vs. $r = 0.55$), we concluded that this path must be dependent on the transmission between individual neurons. Given that this difference was small, however, we mostly used electrode-level dynamics for the subsequent analysis, since that level allowed for higher precision (due to larger spike counts).

After burst onset, the subsequent firing rate dynamics were also conserved. We visualized the temporal evolution of superburst dynamics with a phase plot of the aggregate firing rate (in 100 ms sliding windows) during superbursts (Figure 5(a)). The discrete bands
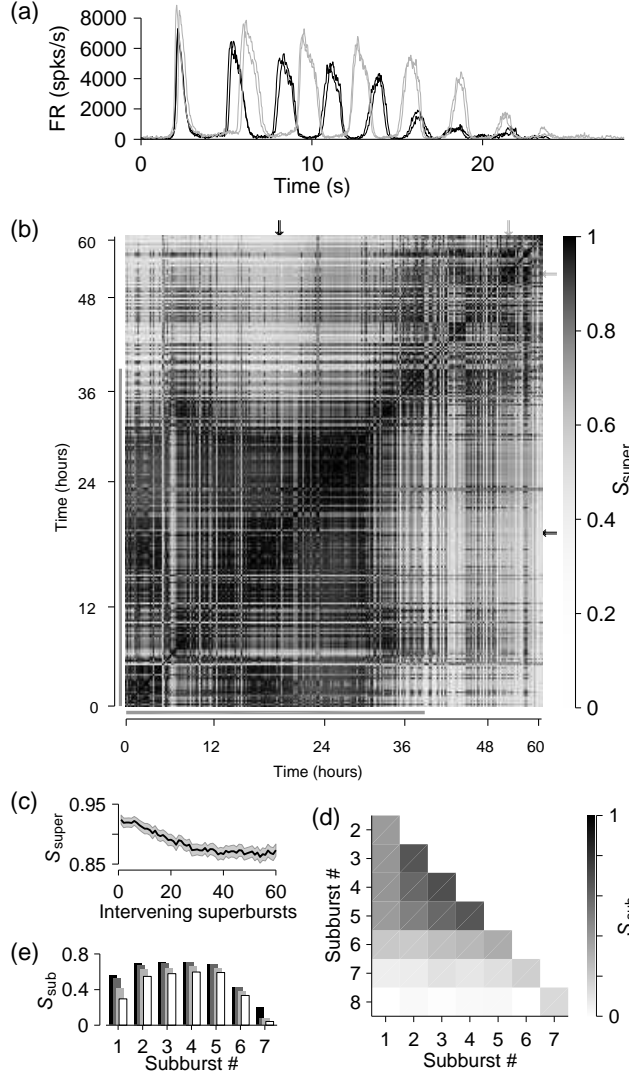
Figure 3: Conservation of firing rates and activity propagation between superbursts. (a) Aggregate firing rates of two pairs (one pair black, one pair gray) of consecutive superbursts separated by 30 hours comprising 150 superbursts (not shown here). While consecutive superbursts are seen to be almost indistinguishable in shape the difference after 30 hours is apparent. (b) A matrix of the global similarity index (S_{super}; see text) between superbursts recorded over a 63 hour period. Two main blocks of strongly conserved similarity can be distinguished. Black and gray arrows mark examples shown in (a). Gray bars mark portion of data used in (c–e). (c) Even with dozens of intervening superbursts, the S_{super} index between superbursts separated by many hours remains very high. (Mean ± SEM for 170 superbursts.) (d) Subburst similarity index (S_{sub}; see text) between bursts within a superburst, averaged over 170 superbursts. A conserved structure is observed between subbursts 2–5. (e) S_{sub} index between homologous subbursts across superbursts. Between consecutive superbursts (black), the 2nd through 5th subbursts are more conserved than the 1st subburst. Between superbursts 30–60 minutes apart (dark gray), 1–2 hours apart (light gray) or 6–24 hours apart (white), this effect is even more pronounced.
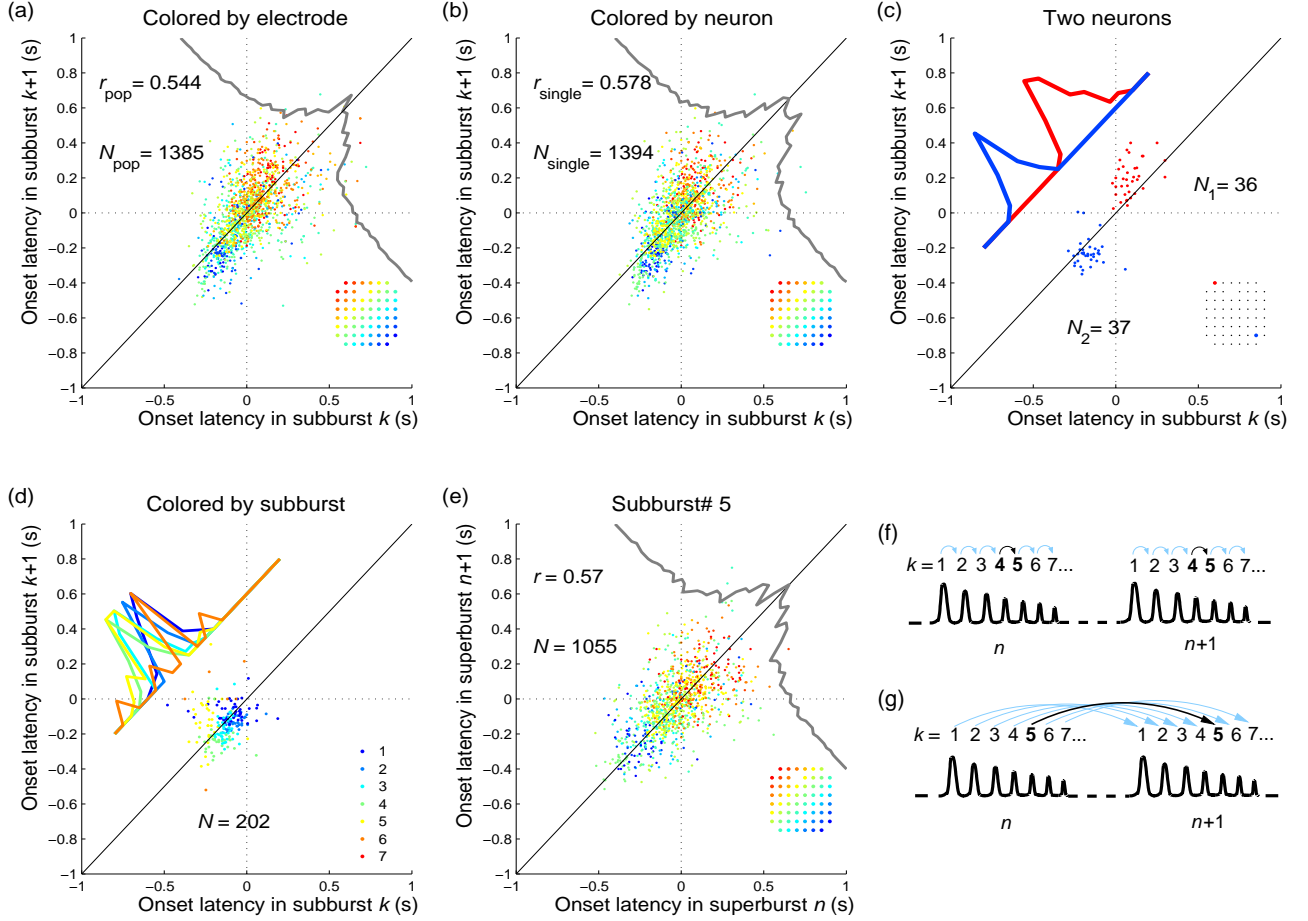
Figure 4: (Color) Return plots (explained in (f)–(g)), representing the temporal structure of burst propagation by recursively plotting the latencies at which a cell or electrode starts to participate in one burst against its latency in the next (or next homologous) burst. (a) Electrode level return plot of burst onset latency from the 4th to the 5th subburst in successive superbursts. The diagonal represents exact latency preservation. Electrodes are color-coded according to the inset. (b) The same return plot as in (a), but instead of combining all spikes from a given electrode, we isolated the most active single unit from each electrode. Color code as in (a). Note how closely the single-unit activity matches the multi-unit activity. (c) The burst onset latency return plot for two neurons, extracted from (b). One neuron (blue) was selected that tended to burst early, and one (red) that tended to burst late. Inset shows the locations of the two neurons. (d) Single-neuron return plots of burst latency across different subbursts, for the blue neuron in (c). Interval number is color-coded. (e) Single neuron level return between the 5th component-bursts across successive superbursts. (f–g) Explanation of return plots: (f) In (a)–(d), features of successive subbursts within a superbursts are compared; (g) In (e), features of homologous subbursts of successive superbursts are compared.

11

formed by the orbits of homologous subbursts are signatures of the distinctive propagation dynamics that consistently recur with each superburst. The systematic variation of subburst trajectories suggests that the generation of superbursts is determined by a higher order attractor that unfolds in different well-defined propagation patterns for each subburst. The reproduction of the same dynamics in each subsequent superburst cannot be explained by intrinsic oscillatory features of individual neurons. Instead, the reproduction depends on the state of the whole network, which imposes on each neuron a precise input configuration that regenerates via recurrent connections. The bands formed by the 2nd through 5th subbursts were much closer together than the band of the 1st subbursts, re-affirming that the initial stages of the superbursts were variable, while subsequent bursts self-organized into a precise temporal pattern—a dynamic attractor—that was stable for hours or days.

All measures discussed so far focus on the temporal structure of the observed recurring activity patterns, and do not speak directly to their spatial structure. For a simple metric of the spatial aspects of superburst dynamics, we defined the horizontal differential firing rate of a culture as the aggregate firing rate in the right half of the array minus the aggregate firing rate in the left half of the array (in 200-ms sliding windows). A vertical differential firing rate was analogously defined. The orbits of superbursts in the state space of differential firing rates show that the preservation of burst shape increases from the 1st to 5th subbursts (Figure 5(b)). The 6th subbursts, which mark the end of the superburst structure for this culture, have orbits of distinctly different shapes than the earlier subbursts.

IV. DISCUSSION

The locations and connectivity of neurons in culture, at least at the the outset, is random. This is a consequence of the method of dissociation and seeding onto the substrate; we made no efforts to create defined structure in the networks, e.g., by using patterned or micromachined substrates as others have [27–30]. The assumption has been that activity in such 'random' networks will likewise be without coherent structure. Nevertheless, self-organization of activity patterns into a two-level structure of subbursts and superbursts was consistently observed (Table I). While superbursts appeared at irregular intervals, their internal structure was highly regular and strongly conserved for hours or days: once a superburst had been initiated, it generated a constant number of subbursts that each had its
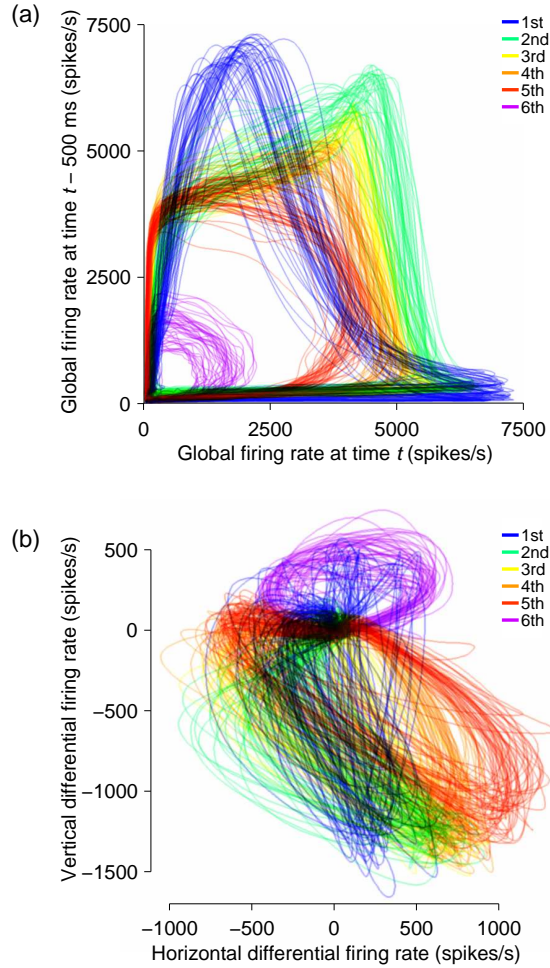
Figure 5: (Color) Spatiotemporal structure of superbursts. (a) Phase plots of the aggregate firing rate for 50 consecutive superbursts. The delay, 500 ms, is short enough to not mix subbursts. The sequential order of trajectories is indicated by different colors. (b) X–Y plot of differential firing rate (see text) for the same 50 superbursts.

own well-preserved geometry of propagation and temporal dynamics. This preservation was found to be precise at the single-neuron level. The spontaneous occurrence of superbursts shows that neurons and glia retain an ability to self-organize into multicellular ensembles with non-trivial functional structure, even when taken out of their physiological context.

Bursting has been described in dissociated cortical culture (e.g. [17, 19, 31–38]), but previously described bursts did not exhibit the two-level structure of superbursts. In MEA recordings from dissociated cultures of neonatal rat cortex, Segev et al. [37] found bursts that clustered into several distinct types based on their spatiotemporal substructures, and that these substructures were reproduced with high fidelity over several hours. We similarly find

conservation of the spatiotemporal substructrue of bursts, but in addition find conservation of sequence: Figure 5 shows that the substructures of all subbursts at a given ordinal position in their superbursts are similar to each other, and distinct from those at different positions. Interestingly, in cortical slices, a different kind of bursts has been observed, at a shorter time scale, governed by a critical branching process reminiscent of avalanches [12]. These bursts consisted of precisely defined firing patterns lasting tens of milliseconds. A given slice could exhibit several different patterns, each of which was conserved for multiple hours [13]. Given the disparity of time scales, both kinds of bursts could in principle co-exist in the activity patterns of a neuronal ensemble, although we have no evidence of preserved firing sequences on a millisecond scale in our cultures.

In vivo, short conserved patterns of activity have been described in several preparations, in terms of action potentials [5, 6], or intracellular calcium increases [11, 14], and fixed-point attractors have been observed in the form of up/down state transitions [39]. Superbursts constitute much longer and more detailed patterns, and are among the longest conserved activity patterns observed in any neural system to date. In *in vivo* experiments, such patterns may have remained hidden because only a small fraction of the neurons from a large ensemble were monitored, or because recordings were too short. By contrast, the use of dissociated cultures permitted us to monitor and evenly sample an entire intact network for weeks.

The coordination of cellular dynamics at the superburst level indicates that information is maintained by a global dynamic process which persists orders of magnitude longer than the time constants of synaptic processing. This allows the information to be protected from the interference of local processing: individual neurons can engage in multiple functions without disrupting the recurring motif reverberating in the larger-scale circuitry of the culture. Such globally organized and tightly orchestrated activity is of critical importance for any neuronal tissue that generates highly stereotyped sequential behaviors, from locomotion to language. The same mechanism may also support a sensory persistence and memory that does not require synaptic plasticity. *In vitro* systems are ideal for studying in detail the conditions that allow such activity patterns to emerge, and for testing mathematical models of neuronal pattern generation at a population level with cellular precision. Moreover, the robustness of the complex pattern generation behavior can open avenues for computation and artificial intelligence applications such as controlling hybrid neural-robotic systems [40–

42]. We are currently experimenting with triggering superbursts with electrical stimulation [43], and initial results look promising. A critical issue for future study is whether an electrical stimulation paradigm can be used to modify the attractors in a controlled manner, as required for learning [44].

Acknowledgments

---

[1] H. R. Wilson and J. D. Cowan, Kybernetik **13**, 55 (1973).

[2] D. J. Amit, *Modeling brain function: The world of attractor neural networks* (Cambridge University Press, 1989).

[3] X. J. Wang, Trends in Neurosci. **24**, 455 (2001).

[4] D. O. Hebb, *The organization of behavior: A neuropsychological theory* (John Wiley and Sons, New York, 1949).

[5] Y. Prut, E. Vaadia, H. Bergman, I. Haalman, H. Slovin, and M. Abeles, J. Neurophysiol. **79**, 2857 (1998).

[6] Z. Nádasdy, H. Hirase, A. Czurkó, J. Csicsvari, and G. Buzsáki, J. Neurosci. **19**, 9497 (1999).

[7] M. Abeles, *Corticonics: Neural circuits of the cerebral cortex* (Cambridge University Press, 1989).

[8] M. Stopfer, V. Jayaraman, and G. Laurent, Neuron **39**, 991 (2003).

[9] M. Rabinovich, A. Volkovskii, P. Lecanda, R. Huerta, H. D. I. Abarbanel, and G. Laurent, Phys. Rev. Lett. **87**, 068102 (2001).

[10] A. Leonardo and M. S. Fee, J. Neurosci. **25**, 652 (2005).

[11] Y. Ikegaya, G. Aaron, R. Cossart, D. Aronov, I. Lampl, D. Ferster, and R. Yuste, Science **304**, 559 (2004).

[12] J. M. Beggs and D. Plenz, J. Neurosci. **23**, 11167 (2003).

[13] J. M. Beggs and D. Plenz, J. Neurosci. **24**, 5216 (2004).

[14] J. N. MacLean, B. O. Watson, G. B. Aaron, and R. Yuste, Neuron **48**, 811 (2005).

[15] H. Kamioka, E. Maeda, Y. Jimbo, H. P. C. Robinson, and A. Kawana, Neurosci. Lett. **206**, 109 (1996).

[16] R. Segev, M. Benveniste, E. Hulata, N. Cohen, A. Palevski, E. Kapon, Y. Shapira, and E. Ben-Jacob, Phys. Rev. Lett. **88**, 118102 (2002).

[17] J. Van Pelt, M. A. Corner, P. S. Wolters, W. L. C. Rutten, and G. J. A. Ramakers, Neurosci. Lett. **361**, 86 (2004).

[18] M. H. Droge, G. W. Gross, M. H. Hightower, and L. E. Czisny, J. Neurosci. **6**, 1583 (1986).

[19] D. A. Wagenaar, J. Pine, and S. M. Potter, BMC Neurosci. **7**, 11 (2006).

[20] C. Y. Chiu and M. Weliky, J. Neurosci. **21**, 8906 (2001).

[21] M. J. O'Donovan, Curr. Opin. Neurobiol. **9**, 94 (1999).

[22] D. Contreras, A. Destexhe, T. J. Sejnowski, and M. Steriade, J. Neurosci. **17**, 1179 (1997).

[23] P. J. Magill, A. Sharott, J. P. Bolam, and P. Brown, J Neurophysiol. **92**, 2122 (2004).

[24] S. M. Potter and T. B. DeMarse, J. Neurosci. Meth. **110**, 17 (2001).

[25] R. Q. Quiroga, Z. Nadasdy, and Y. Ben-Shaul, Neural Comput. **16**, 1661 (2004).

[26] D. A. Wagenaar, T. B. DeMarse, and S. M. Potter, in *Proc. 2nd Intl. IEEE EMBS Conf. on Neural Eng.* (2005), pp. 518–521.

[27] P. Clark, P. Connolly, A. S. Curtis, J. A. Dow, and C. D. Wilkinson, Development **99**, 439 (1987).

[28] D. Kleinfeld, K. H. Kahler, and P. E. Hockberger, J. Neurosci. **8**, 4098 (1988).

[29] D. W. Branch, J. M. Corey, J. A. Weyhenmeyer, G. J. Brewer, and B. C. Wheeler, Med. Biol. Eng. Comput. **36**, 135 (1998).

[30] D. A. Stenger, J. J. Hickman, K. E. Bateman, M. S. Ravenscroft, W. Ma, J. J. Pancrazio, K. Shaffer, A. E. Schaffner, D. H. Cribbs, and C. W. Cotman, J. Neurosci. Methods **82**, 167 (1998).

[31] Y. Jimbo, H. P. C. Robinson, and A. Kawana, IEEE Trans. Biomed. Eng. **40**, 804 (1993).

[32] P. E. Latham, B. J. Richmond, S. Nirenberg, and P. G. Nelson, J. Neurophysiol. **83**, 828 (2000).

[33] R. Segev, Y. Shapira, M. Benveniste, and E. Ben-Jacob, Phys. Rev. E **64**, 011920 (2001).

[34] T. Opitz, A. D. De Lima, and T. Voigt, J. Neurophysiol. **88**, 2196 (2002).

[35] T. Tateno, A. Kawana, and Y. Jimbo, Phys. Rev. E **65**, 051924 (2002).

[36] D. A. Wagenaar, R. Madhavan, J. Pine, and S. M. Potter, J. Neurosci. **25**, 680 (2005).

[37] R. Segev, I. Baruchi, E. Hulata, and E. Ben-Jacob, Phys. Rev. Lett. **92**, 118102 (2004).

[38] E. Hulata, I. Baruchi, R. Segev, Y. Shapira, and E. Ben-Jacob, Phys. Rev. Lett. **92**, 198105 (2004).

[39] R. Cossart, D. Aronov, and R. Yuste, Nature **423**, 283 (2003).

[40] D. J. Bakkum, A. C. Shkolnik, G. Ben-Ary, P. Gamblen, T. B. DeMarse, and S. M. Potter, in *Embodied Artificial Intelligence*, edited by F. Iida, L. Steels, and R. Pfeifer (Springer-Verlag, 2004), pp. 130–145.

[41] Z. C. Chao, D. J. Bakkum, D. A. Wagenaar, and S. M. Potter, Neuroinformatics **3**, 263 (2005).

[42] T. B. DeMarse, D. A. Wagenaar, A. W. Blau, and S. M. Potter, Auton. Robots **11**, 305 (2001).

[43] D. A. Wagenaar, J. Pine, and S. M. Potter, J. Neurosci. Meth. **138**, 27 (2004).

[44] G. Shahaf and S. Marom, J. Neurosci. **21**, 8782 (2001).

[45] See EPAPS Document No. [*number will be inserted by publisher*] for a movie showing an example of a superburst in real-time. For more information on EPAPS, see http://www.aip.org/pubservs/epaps.html.